

Effect of Chimney Configurations on Air Flow Rate

Elshafei Bedir Zeidan¹, Ahmed Abdel Razik Ahmed Sultan², Alaa Abdulmunem Lateef³

¹Assistant Professor, Department of Mechanical Engineering, Faculty of Engineering, Mansoura University, Egypt

²Professor of Mechanical Power, Department of Civil Engineering, Faculty of Engineering, Mansoura University, Egypt

³Post Graduate Student at Faculty of Engineering, Department of Mechanical Engineering, Faculty of Engineering, Mansoura University, Egypt

Abstract: *This paper studies the effect of some of the variables on the rate of air flow through the chimney. A test table consisting of an electrically heated base was replaced and replaced by solar energy and a solar chimney was placed on top of it. Both the height of the chimney - the diameter of the chimney - the ratio of chimney diameters and the area of the base surface have been changed. From the study, it was found that the air flow rate, the heat transfer coefficient and the number of Nusselt were increased with both the heat flux density and the modified Rayleigh number. Also, from the practical results it was concluded that the amount of air flowing through the chimney increases with increasing chimney height and decreasing chimney diameter as the amount of air flow decreases at Changing the ratio of the diagonal of the chimney at a fixed height. Also, it is possible from the results to conclude that the amount of air flowing through the chimney increases with an increase in the ratio of the area of the heated base to the diameter of the chimney.*

Keywords: Solar energy, Modified Rayleigh number, Heat flux density

1. Introduction

The increases in oil prices and energy demand combined with recent environmental constraints have rapidly increased the global demand for renewable energy. Solar energy is one of the most promising solutions, especially considering its technological advancements and its growth in the recent years. One of the options that will help meet these demands is the solar chimney power plant (SCPP). The SCPP is a proposed type of renewable-energy power plant that transforms solar energy into electricity.

2. Literature Review

Bernardes et al. (2003) developed an analytical and numerical model for a solar chimney power plant, comparing simulation predictions to experimental results from the pilot plant at Manzanares.

Chergui et al., (2010) created a model with no turbine or thermal storage system to isolate and observe the air movement within the system. The air flow was controlled by the boundary conditions. After a temperature difference was calculated using the Rayleigh number equation, the lower temperature was set to the chimney walls and the higher temperature was set to the ground. The difference affected the flow dramatically.

Huang et al., (2007) Simulated The main factors that influence on the performance of the SCPPS. The effects on the flow field of the SCPPS which caused by solar radiation intensity have been analyzed. The calculated results are approximately equivalent to the relative experimental data of the prototype. It showed the dependability of the simulative results and the validity of the simulation methods.

Hanna et al., (2016), presented a study on a system constructed to evaluate the performance of the solar chimney turbine and power generation characteristic in the hottest site where of Aswan located at the nearest of the Tropic of

Cancer at the summer season. Velocity, electric power generation and the turbine efficiency were studied in this work. The numerical analyses were performed by using a commercial code CFX, ANSYS 16.1 to simulate the flow through the turbine and overall system. The study showed that the range power generated was (1.2 W - 4.4 W).

Kirstein and Backstrom, (2006) performed numerical analysis to study the flow through a solar chimney power plant SCPP collector-chimney transition section using commercial CFD software, ANSYS-CFX. CFX used to verify the experimental data of a scaled model SCPP. Due to the very good agreement between the experimental and numerical results, CFD software can be used to predict the performance of a full sized SCPP.

Ming et al. (2006), presented a mathematical model to evaluate the relative static pressure and driving force of the solar chimney power plant system and verified the model with numerical simulations. Later, they developed a comprehensive model to evaluate the performance of a solar chimney power plant system, in which the effects of various parameters on the relative static pressure, driving force, and efficiency have been further investigated.

Pasthor et al. (2004) carried out a numerical simulation to improve the description of the operation mode and efficiency by coupling all parts of the solar chimney power plant including the ground, collector, chimney, and turbine.

Stojkovski et al, (2016) presented a study involving mathematical modelling of the system, based on the computational fluid dynamics (CFD) approach. The technical features of solar chimney power plant were analyzed by use of CFD technique, as a way for effective optimization of the object's geometry and thermo-fluid aspects. The created numerical domain represented the complete volume of the object under consideration, with total height of 100 m, chimney's-based radius of 6.25 m,

chimney's top radius of 10.5 m and roof radius of 100 m. The numerical grid consisted of 276000 volume cells, 729242 faces and 190156 nodes. The governing equations for mass, momentum and energy were solved using a commercial CFD code.

Zhou, (2007) presented experiment and simulation results of a solar chimney thermal power generating equipment in China, based on the simulation and the specific construction costs at a specific site, the optimum combination of chimney and collector dimensions was selected for the required electric power output.

3. Experimental Apparatus and Instruments

In order to investigate experimentally the effect of different parameters on ventilation rate of air, a test rig is designed and manufactured in Mechanical Power Engineering Department, Faculty of Engineering, Mansoura University.

The test rig shown in Fig.(1-a) consists of the test section, variable transformer (6), ammeter (5), volt meter (4), temperature measuring device (7), thermocouples measuring air temperature out of the duct (2), thermocouple measuring temperature air surrounding the duct (12), thermocouples measuring the temperatures on the pallet (9,10,11), power supply source (6), the assembly cone (8), the thermo anemometer (1), the ammeter (5) the air duct heaters distributed, (13,14) and wiring system type (VEYRON VL9205 digital multi-meter measures electric current ranged from 0.0 to 20 A, with a minimum reading of 2mA and accuracy of ±1.2%. The voltmeter (4) type (VEYRON VL9205 digital multi-meter) measures electric volts ranged from 0.0 to 200 V, and an accuracy of ±1.2 %.

The variable transformer (6) type (TROIDAC) capable of providing electric volts from 0.0 to 380 volts was used. The temperature measuring device is a temperature recorder type (YOKOGAWA) with 24 channels capable of reading and recording the temperature reading of different thermocouple types (K and R) with a minimum reading of 0.1°C and an accuracy of ± 0.3 %.

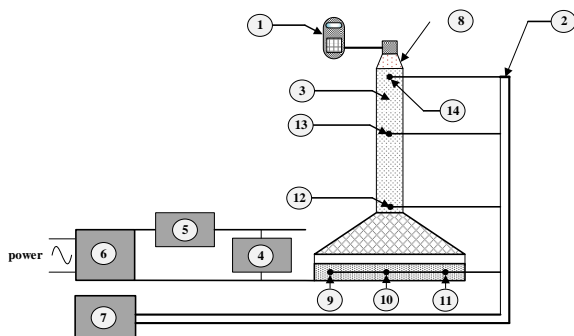


Figure 1: Schematic diagram of the experimental setup

- 1- Thermo anemometer
- 2- Thermos couples
- 3- Tube air
- 4- Volt meter (V)
- 5- Amperemeter (I)
- 6- Variac variable transformer
- 7- Temperature recorder
- 8- Assembly cone

- 9,10,11,12 -Thermocouples
- 13,14 – Air duct heaters distributed

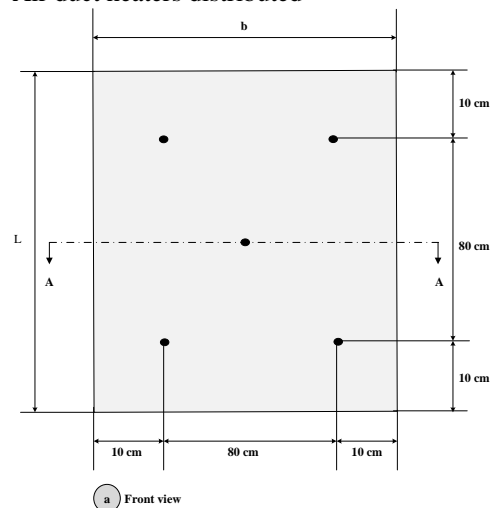


Figure 2: Thermocouples probe distribution over heater plate

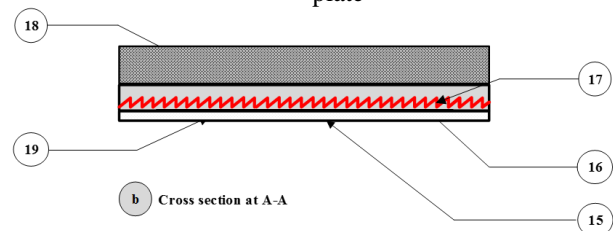


Figure 3: Cross-section of heater assembly

4. Experimental Procedure

Before starting the experiments, the following steps are made:

- 1) Connect thermocouples leads to the temperature recorder;
- 2) Connect the heater leads to the transformer via ammeter and voltmeter;
- 3) Connect the transformer to the main electric supply;
- 4) Regulate the transformer to the predetermined voltage;
- 5) Open the electric circuit and let the system working until it reaches the steady state condition by monitoring the mean heated surface temperature;
- 6) When the system reaches the steady state, condition register the readings of all connected thermocouples, the volt meter, amperemeter, and finally the Anemometer reading;
- 7) Changing the transformer exit voltage to a higher value of power and repeat the steps 5 and 6.

The heat flux density (q) added to the system can be calculated as:

$$q = (I \times V) / A \quad (1)$$

where I is the current in ampere, V volt and A is the area of the heated plate in m².

5. Results and Discussion

Seven parameters discussed in this work are heat flux density (q), heat transfer coefficient (H), pipe height (h), diameter (D), angles (θ), gap thickness(δ), heater area(A)

5.1 Effect of tube height

Fig. (4) represents the relation between air mass flow rate and heat received with vertical cylinder diameter of (16 cm) and height ranging from 100 cm to 300 cm. From the Fig. one can conclude that air flow rate increases with cylinder height and heat received. This is may be due to chimney effect and air mean temperature respectively.

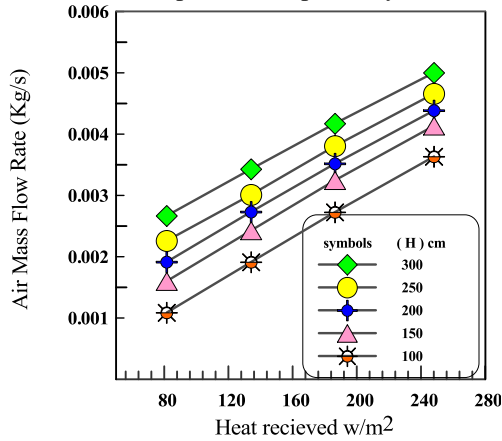


Figure 4: Relation between heat flux density and air mass flow rate for tube with diameter (16 cm) and different height

5.2 Effect of tube diameter

Fig. (5) illustrates the relation between air mass flow rate and heat received with vertical cylinder of 200 cm height and different diameters of 2,3 and 4 in (\approx 5,7.5 and 10 cm). The figure shows that air flow rate increases with cylinder diameter and heat received. This is may be due to the decrease pressure pantry loss with the increase of cylinder diameter.

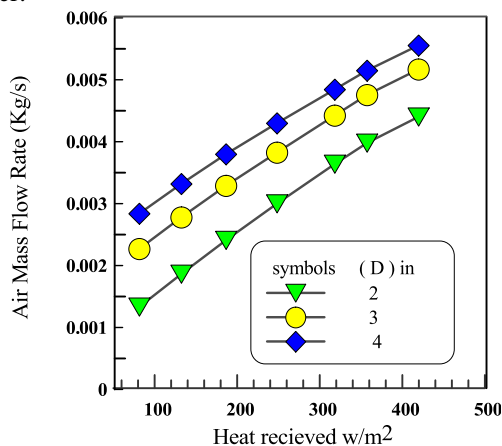


Figure 5: Relation between heat flux density different diameters

5.3 Effect of tube angles

Fig. (6) indicates the relation between air mass flow rate and heat received with conical tube of 100 cm height and angles of cone of 0, 1.14, 1.71, 2.29, 2.86 and 3.34. The figure shows that air flow rate increases as the cone angle decreases.

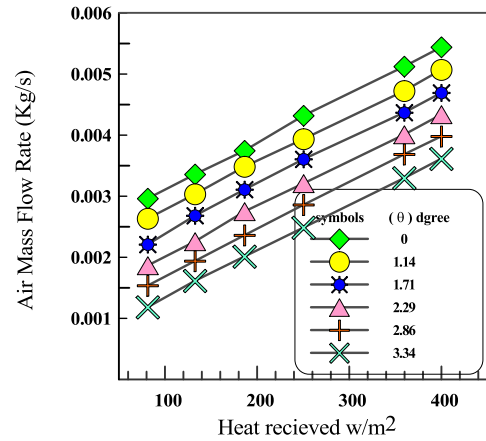


Figure 6: Relation between heat flux density and air mass flow rate for tube of height (1 m) at different radii ratio for gap thickness (7 cm)

5.4 Effect of gap thickness

Fig.(7) Shows the relation between air mass flow rate and heat received with vertical cylinder of height 200 cm and different inlet gap thickness 10,15,20 and 25 cm .From the figure (6) it is concluded that air flow rate increases with the decrease of inlet gap thickness .This may be because, for the same heat received, the inlet velocity increases with the decrease of gap thickness. This in turns enhance the heat transfer from plate surface y_0 air and consequently increases the amount of heated air.

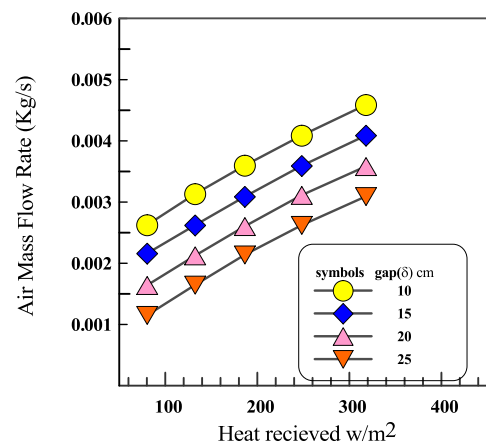


Figure 7: Relation between heat flux density and air mass flow rate for tube of height (2 m) at different gap thickness at inlet

5.5 Effect of heated plate area

Fig. (8) Represents the relation between air mass flow rate and heat received with vertical cylinder diameter at (200 cm) and different diameters (5, 10, 10 cm) with heated plate area of (1.25 m2). The figure shows that air flow rate increases with the diameter of the cylinder and heat received.

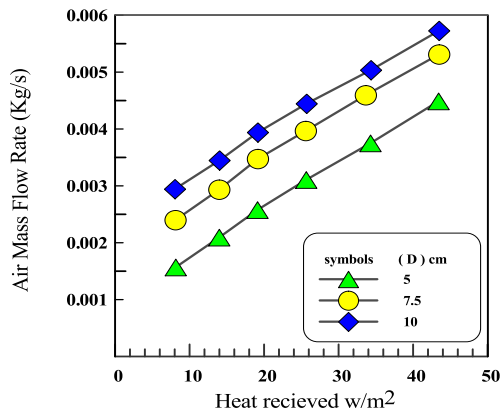


Figure 8: Relation between heat flux density and air mass flow rate for cylinder with height (200 cm) and different diameters with area (1.25 m²)

5.6 Effect of heat transfer coefficient

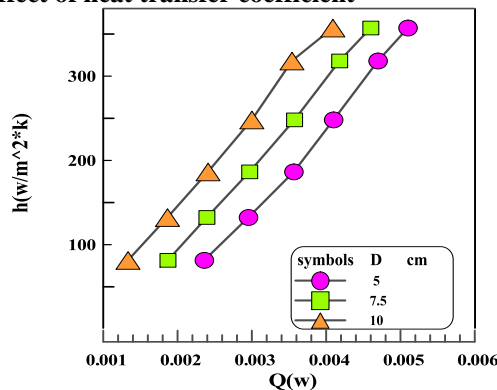


Figure 9: Relation between heat transfer coefficient (h) and heat flux (Q) for H = 200 cm, D = (5, 7.5 and 10) cm

5.7 Effect Modified Rayleigh number on Nusselt number

Fig. (10) Shows the relation between Nusselt number and modified Rayleigh number with vertical cylinder of 200 cm height and diameters of 2, 3 and 4 in. The figure shows that Nusselt number increases with the cylinder diameter and heat received.

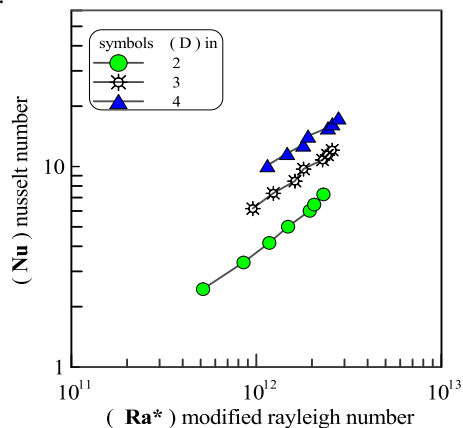


Figure 10: Relation between Nusselt number (Nu) and modified Rayleigh number (Ra) for h=200 cm and base area of (1 m²)

6. Experimental Procedure

From the above results the following conclusions can be made:

- 1) The air flow rate increases with cylinder height and diameter of tube.
- 2) The air flow rate decreases with angles of cone, gap thickness, heated plate area and heat received.

Nomenclature

- A Surface area of the heated side, m²
- A_a cross section area of anemometer fan, m²
- v Anemometer velocity reading, m/s
- h_h Heated surface height, m
- h_t Tube height, m
- I Electric current, Ampere
- V Electric volt, volt
- q heat flux density, W/m²

References

- [1] Bernardes, A., Dos, S. Weinrebe, G., 2003 - Thermal and technical analyses of solar chimneys. Solar Energy 75 (6), 511–524
- [2] Chergui T., Larbi S., and Bouhdjar A., 2010 - Thermo-hydrodynamic aspect Analysis of Flows in Solar Chimney Power Plants-A Case Study, Renewable and Sustainable Energy Reviews (14), pp. 1410 - 1418.
- [3] Huang, H., et al., 2007-Simulation Calculation on Solar Chimney Power Plant System, Challenges of Power Engineering and Environment, 1 ,14, pp. 1158-1161.
- [4] Hanna M. et al., 2016 - Experimental and Numerical Investigation of the Solar Chimney Power Plant’s Turbine. Faculty of Engineering, Mechanical Power and Energy Department, Minia University, Aswan University, Egypt. Open Journal of Fluid Dynamics, 2016, 6, 332-342.
- [5] Kirstein F., Backstrom T., 2006- Flow through a solar chimney power plant collector-to-chimney transition section. J Sol Energy Eng, 2006.pp:128-317.
- [6] Ming, T. Z., Liu, W., Xu, G. L.,2006 - Study of the Solar Chimney Power Plant Systems, J Eng Thermodynam, 27 (2006), 3, pp. 505-507
- [7] Pasthor, H., Kornadt, O., Gurlebeck, K., 2004-Numerical and Analytical Calculations of the Temperature and Flow Field in the Upwind Power Plant, Int J Energy Res, 28 (2004), 6, pp. 495-510.
- [8] Stojkovski F, et al., 2016- Numerical Modelling of a Solar Chimney Power Plant, International Journal of Contemporary ENERGY, Vol. 2, No. 1 (2016) ISSN 2363-6440, pp:14-21.
- [9] Zhou, X., et al., 2007- Simulation of a Pilot Solar Chimney Thermal Power Generating Equipment, Renew Energy, 32 (2007), 10, pp. 1637-1644

Author Profile



Elshafei Bedir Zeidan received BSC & MSC from Mansoura University, Mansoura, Egypt. PhD from University of Victoria, Victoria BC, Canada. Lecturer at Mansoura University since 1998.



Ahmed Abdel Razik Ahmed Sultan received the B.S. and M.S. degrees in Mechanical Power from Mansoura University in 1974 and 1980, respectively. Ph.D. Odessa Technological Institute for Refrigeration industries. YKRANIA.USSR(1987) Administrator at

Mansoura University, from 1974 to 1980. Teaching assist at Mansoura university, from 1980 to 1987. Lecturer at Mansoura university, from 1987 to 1994. Assist. prof. at Mansoura university since 1994.



Alaa Abdulmunem Lateef received B.S. from Anbar University / Mechanical Power Engineering Department in 2003. Lecturer at the Technical Institute / Middle Technical University for the academic year 2005-2004. Employee in the construction and projects department / Wasit University since 2005.